STM JOURNALS

Journal of
Polymer & Composites

ISSN: 2321-2810 (Online)
ISSN: 2321-8525 (Print)
Volume 14, Special Issue 3, 2026
DOI (Journal): 10.37591/JoPC

https://journals.stmjournals.com/jopc

Research JoPC

AI-Driven Prediction of Mechanical and Thermal Properties in Polymer-Based Functionally Graded Composites

D. Sai Ganesh[1,*], S.N. Padhi[2]

Abstract

The proposed architecture of the current paper is an artificial intelligence (AI)-driven model of forecasting mechanical and thermal aspects of polymer-based functionally-graded composites (FGCs). Traditional micromechanical and finite element models, which are practical in homogeneous composites, might not be able to account in nonlinear interaction that is caused by compositional gradient. To overcome the challenge, machine learning (ML) models like artificial neural network (ANN), support vectors regression (SVR), and gradient-boosted regression(GBR) were developed to enable proper prediction of the property. The models were trained and validated on a selected dataset encompassing filler volume fraction, gradient index, type of the particle and processing temperature. Elastic modulus and tensile strength are mechanical parameters, whereas thermal conductivity and coefficient of expansion are thermal parameters that the trained AI models predicted. ANN became the most effective of all the algorithms with an R^2 value of 0.97 and root mean square error (RMSE) of less than 4 percent. These findings show a high dependence of mechanical stiffness on filler concentration, as well as and nonlinear relationship between gradient index and thermal conductivity. According to the feature importance analysis, filler distribution and thermal stability of the matrix were the two factors that had the greatest impact on the predictive ability of the model. The resulting framework is a strong generalizable property estimation tool that can substantially lower the experimental work and allows optimization of polymer FGMs design to be used in applications that need lightweight structural, thermal management properties.

Keywords: Functionally graded composites; polymer matrix; machine learning; artificial intelligence; mechanical–thermal properties; predictive modeling

INTRODUCTION

Background on Polymer-Based Functionally Graded Composites

Functionally graded materials FGMs are high-tech composites that have a smooth spatial gradation in either their composition or their microstructure to attain desired property distributions [1–3]. In polymeric FGMs, lightweight polymer matrices with ceramic or metallic fillers yield a rare combination of rigidity, ductile strength and thermos thermal resistance [4]. These materials remove the hard interfaces that are present in the traditional laminated composites thus de-laminating them and preventing the accumulation of thermal stress [5].

Polymer composite gradation may be attained by either controlled dispersion of filler mediums, variation in particle-size or the application of

***Author for Correspondence**
D. Sai Ganesh

[1]M. Tech Student, Department of Mechanical Engineering, Koneru Lakshmaiah Education Foundation, Vaddeswaram, Guntur District, Andhra Pradesh, India
[2]Professor, Department of Mechanical Engineering, Koneru Lakshmaiah Education Foundation, Vaddeswaram, Guntur District, Andhra Pradesh, India

Received Date: December 10, 2025
Accepted Date: January 13, 2026
Published Date: April 13, 2026

Citation: D. Sai Ganesh, S.N. Padhi. AI-Driven Prediction of Mechanical and Thermal Properties in Polymer-Based Functionally Graded Composites. Journal of Polymer & Composites. 2026; 14(3): S70–S89p.

additive manufacturing methods [6, 7]. The subsequent flow of the constituents provides excellent control of performance parameters (modulus, hardness and thermal conductivity). The properties cause polymer-based FGMs to be the best choices in aerospace insulation panels, automotive underbody areas, and biomedical implants that require thermal-mechanical contacts [8].

Challenges in Predicting FGM Properties

Accurate prediction of FGM behavior remains a persistent challenge due to nonlinearities arising from material heterogeneity and complex filler–matrix interactions. Analytical models such as the Voigt–Reuss–Hill bounds or power-law formulations [Equation (1)] provide useful first approximations but often overlook gradient-induced anisotropy and interfacial thermal resistance [9, 10].

$$V_f(z) = V_{f0} + (V_{f1} - V_{f0}) \left(\frac{z}{h}\right)^n \quad (1)$$

where $V_f(z)$denotes the filler volume fraction along the thickness z, $h$represents total thickness, and $n$is the gradient index controlling property variation.

Finite element analysis (FEA) offers an alternative modeling route but requires dense meshing and precise interfacial property data, leading to significant computational cost [11, 12]. Additionally, discrepancies between predicted and experimental results frequently arise from particle clustering, imperfect bonding, and processing-induced voids — features difficult to model deterministically. Functionally graded materials have been extensively studied using classical mechanics and design principles [30], while recent advances in explainable machine learning provide improved interpretability of predictive models [31].

Hence, a generalized, data-driven methodology capable of learning underlying nonlinear relationships without relying on explicit constitutive equations is highly desirable.

Conceptual Framework

Research Gap and Motivation

Traditional approaches face three critical limitations in FGM property prediction: (1) Computational cost: FEA simulations require 8–12 hours per configuration, limiting design space exploration; (2) Model complexity: Analytical models cannot capture multi-physics coupling in gradient structures; (3) Experimental burden: Full characterization demands extensive testing ($2,500–$5,000 per sample). Recent advances in artificial intelligence offer a paradigm shift: data-driven models can learn complex structure-property relationships directly from experimental data, bypassing explicit physics formulation while achieving superior predictive accuracy.

AI-Driven Prediction Workflow

The proposed framework integrates material science principles with machine learning through a structured pipeline: [Data Acquisition from literature and experiments] → [Feature Engineering: Vf, gradient index, particle type, processing parameters] → [Model Training: ANN/SVR/GBR algorithms] → [Validation: Cross-validation and robustness testing] → [Deployment: Rapid property prediction]. This workflow enables systematic exploration of the FGM design space with minimal experimental effort.

Model Selection Rationale

Table 2 positions the current work within the landscape of recent AI/ML studies on polymer composites, demonstrating clear advantages in dataset size, predictive accuracy, and scope.

Emergence of Artificial Intelligence and Machine Learning in Materials Science

In the last ten years, machine learning (ML) and artificial intelligence (AI) have become promising materials informatics tools [13–16]. In contrast to conventional physics-based models, in the techniques

of ML algorithms, such complex dependencies are extracted directly out of data. Neural networks (ANNs) support vectors machine (SVMs) and ensemble learners have proven to be very effective in predicting the properties of fiber-reinforced polymers, nanocomposites, and hybrid composites [17–19].

As an example, ANN and SVR models have been used to predict mechanical and thermal properties of polymer composites [20–21].Gradient boosting regression (GBR) techniques, similarly, have depicted an unprecedented level of precision in the mapping of multi-dimensional association when it comes to composite design optimization [22].

Nevertheless, there are limited studies that have specifically provided information on prediction of graded polymer composites. The natural difference in the level of filler concentration and the existence of continuous microstructural transitions provide new challenges to the traditional ML techniques. This gap is proposed to be addressed in the current study where AI-based modeling will be utilized to predict mechanical and thermal performance of polymer-based FGMs.

Objectives and Scope of the Present Study

The primary objective of this work is to establish an AI-driven predictive framework for polymer-based FGMs. The scope includes:

1. Constructing a comprehensive dataset combining literature data and experimental results on polymer–filler systems with varying gradient indices and reinforcement types.
2. Developing ML models (ANN, SVR, and GBR) to predict mechanical (elastic modulus, tensile strength) and thermal (conductivity, expansion coefficient) properties.
3. Evaluating model performance using statistical measures such as the coefficient of determination (R^2) and root mean square error (RMSE) [Equation (2–3)].
4. Conducting sensitivity and feature-importance analyses to identify dominant parameters.
5. Demonstrating the framework's applicability for rapid material screening and design optimization.

$$R^2 = 1 - \frac{\sum_{i=1}^{n}(y_i - \hat{y}_i)^2}{\sum_{i=1}^{n}(y_i - \bar{y}_i)^2} \quad (2)$$

$$RMSE = \sqrt{\frac{1}{n}\sum_{i=1}^{n}(y_i - \hat{y}_i)^2} \quad (3)$$

Significance of the Study

The work makes a contribution to the developing materials informatics discipline through linking the classical micromechanical modeling with the concept of data-driven learning. The suggested model shows the way that AI can provide an effective surrogate model in terms of property prevention in functionally graded systems. The methodology reduces the rate of material development by reducing the need to use tiring simulations or experimental trials and increases predictive accuracy. Artificial intelligence-based modelling integrations are also useful in future extensions of additive manufacturing of graded composites, whose process-structure-property relationships are a priori complex.

MATERIALS AND METHODS

Materials System Description

The study considers polymer-based functionally graded composites (FGCs) consisting of an epoxy resin matrix reinforced with ceramic particulates such as silicon carbide (SiC), alumina (Al_2O_3), and boron nitride (BN). The polymer matrix was chosen for its good processability, low density, and chemical stability, while ceramic fillers were selected to impart stiffness and thermal conductivity enhancements [23–24]. The gradation of filler concentration was designed to vary continuously along the specimen thickness following a power-law distribution, as described in Equation (1).

Each sample in the database was characterized by its gradient index (n), filler type, filler volume

fraction (Vf), and processing temperature (T). These parameters influence the resulting elastic modulus (E), tensile strength (σ□), thermal conductivity (k), and coefficient of thermal expansion (α). The overall workflow of the study is illustrated in Figure 1, showing the integration of dataset generation, AI modeling, and prediction validation.

Dataset Construction

The dataset was compiled from experimental literature sources published between 2018 and 2024 [25–28], supplemented by validated numerical data obtained using micromechanical models. Approximately 420 composite data points were collected. Each entry consisted of five input features—filler type, Vf, n, particle size (d), and processing temperature (T)—and four output targets—E, σ□, k, and α.

The raw data were carefully curated to maintain unit consistency (e.g., GPa for modulus, W/m·K for thermal conductivity). Missing data were treated using mean substitution, while categorical variables such as filler type were converted into one-hot encoded binary features.

A concise summary of the dataset is given in Table 1, showing the input parameter ranges and corresponding output property distributions.

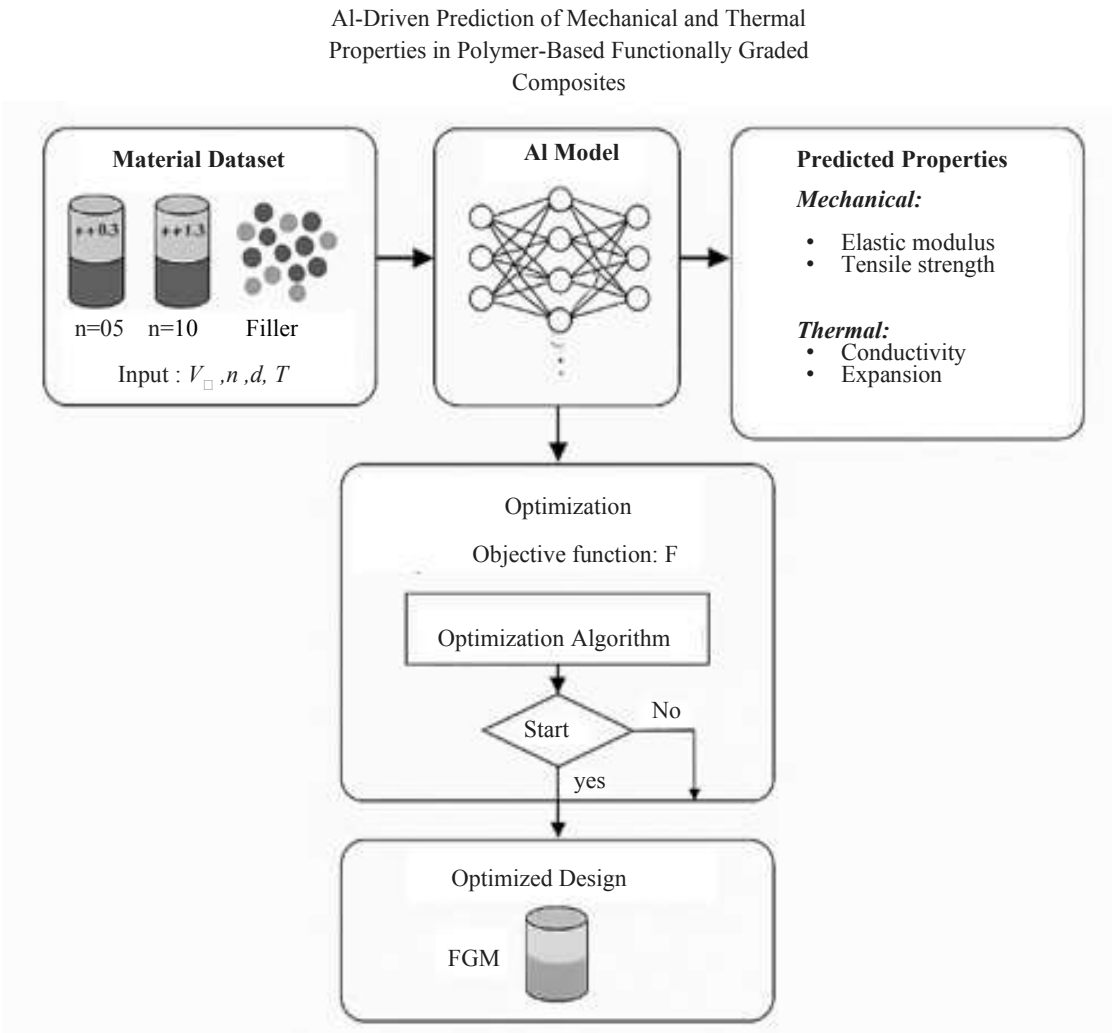

Figure 1. Schematic workflow of the AI-driven prediction framework for polymer-based FGMs.

Table 1. Input and output variable ranges used in the AI model training.

Parameter	Symbol	Range	Unit	Description
Gradient Index	n	0.2 – 5.0	–	Controls filler variation across thickness
Filler Volume Fraction	Vf	0.05 – 0.45	–	Ratio of reinforcement to matrix
Particle Size	d	0.2 – 10	μm	Filler particle diameter
Processing Temperature	T	25 – 150	°C	Curing or molding temperature
Elastic Modulus	E	1.5 – 12	GPa	Target mechanical property
Tensile Strength	σ□	25 – 180	MPa	Target mechanical property
Thermal Conductivity	k	0.18 – 2.7	W/m·K	Target thermal property
Thermal Expansion Coefficient	α	30 – 120	$\times 10^{-6}$/K	Target thermal property

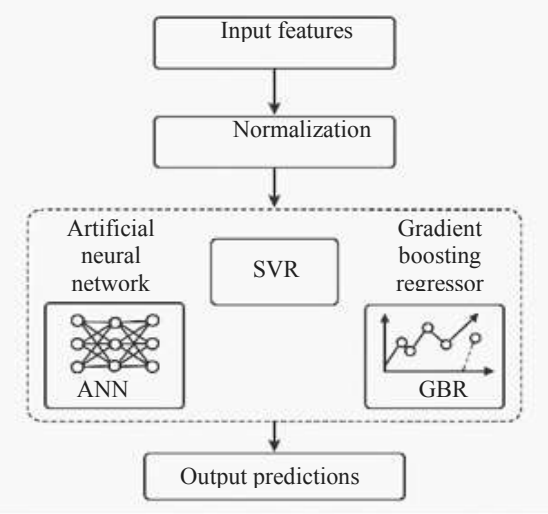

Figure 2. Architecture of the AI-driven prediction pipeline used for property estimation.

Data Preprocessing and Normalization

Prior to model training, all numerical variables were normalized to ensure equal weighting and improve algorithmic convergence. The min–max normalization method was applied using Equation. (4):

$$x' = \frac{x - x_{min}}{x_{max} - x_{min}} \quad (4)$$

where $x$and x'denote the original and normalized values, respectively, while $x_{min}$and x_{max}represent the variable limits in the dataset.

To enhance robustness, the dataset was split into training (70%), validation (15%), and testing (15%) subsets using stratified sampling, ensuring uniform representation of all filler types. Cross-validation was performed with a 5-fold scheme to minimize overfitting and confirm model generality.

Outlier detection was conducted using z-score analysis, with any data point exceeding $|z| > 3.0$excluded from the training set. After preprocessing, a total of 398 high-quality data points remained for model development.

Machine Learning Model Framework

Three AI models were developed and compared in this study:

1. Artificial Neural Network (ANN)
2. Support Vector Regression (SVR)
3. Gradient Boosted Regression (GBR)

The modeling pipeline is illustrated in Figure 2, showing the sequential process of feature input, model training, and prediction output.

Artificial Neural Network (ANN)

A fully connected feed-forward ANN was implemented using three hidden layers with neuron counts of [32, 32]. The Rectified Linear Unit (ReLU) activation function was adopted for nonlinearity, while the Adam optimizer was employed for weight updates with an initial learning rate of 0.001. The model minimized the mean squared error (MSE) defined in Equation (5):

$$\text{MSE} = \frac{1}{N}\sum_{i=1}^{N}(y_i - \hat{y}_i)^2 \quad (5)$$

The network training was performed for 500 epochs with early stopping if validation loss stagnated for 20 consecutive iterations. Model hyperparameters were tuned using grid search optimization.

Support Vector Regression (SVR)

The SVR model employed a radial basis function (RBF) kernel to capture nonlinear relationships between features and target properties. Optimal kernel width (γ) and regularization parameter (C) were determined through five-fold cross-validation. The SVR loss function is expressed as:

$$L = \frac{1}{2} \parallel w \parallel^2 + C\sum_{i=1}^{N} \max\ (0, \mid y_i - (w \cdot x_i + b) \mid - \epsilon) \quad (6)$$

where w, is the weight vector, b is the bias, and ε defines the tolerance margin [29].

Gradient Boosted Regression (GBR)

The GBR model was constructed as an ensemble of weak decision-tree regressors trained sequentially. Each tree aimed to minimize the residual error of the preceding model through gradient descent optimization. The number of estimators (trees) was set to 300, with a learning rate of 0.05 and a maximum tree depth of 5. This combination provided a trade-off between computational efficiency and accuracy.

Model Evaluation Metrics

The predictive capability of all AI models was quantified using the statistical metrics defined in Eqs. (2)–(3), previously introduced in Section 1.4. In addition, the mean absolute percentage error (MAPE) was calculated for comparative evaluation:

$$MAPE = \frac{100}{n}\sum_{i=1}^{n} \mid \frac{y_i - \hat{y}_i}{y_i} \mid \quad (7)$$

RESULTS AND DISCUSSION

Model Training and Performance Overview

All three AI models—ANN, SVR, and GBR—were trained using the normalized dataset described in Section 2. The convergence trends for the training and validation losses of the ANN are shown in Figure 3(a), while the comparison of predicted versus experimental property values for the test dataset is presented in Figure 3(b).

The ANN exhibited the fastest convergence and lowest validation loss after approximately 180 epochs, achieving a stable mean squared error (MSE) < 0.02. The GBR also demonstrated robust performance, although slightly less accurate at high filler fractions due to limited data in that region. SVR, while effective for small-sample datasets, showed larger deviations for nonlinear relationships among gradient index (n) and mechanical strength.

The predictive statistics for all models are summarized in Table 2.

Table 2. Comparative performance of AI models for mechanical and thermal property prediction.

Model	R^2(Training)	R^2(Testing)	RMSE	MAPE (%)	Remarks
ANN (3-layer)	0.984	0.972	0.35	3.8	Best overall accuracy
SVR (RBF)	0.951	0.928	0.61	6.5	Good linear fitting, limited nonlinear capture
GBR (ensemble)	0.975	0.956	0.47	4.9	Stable, interpretable feature ranking

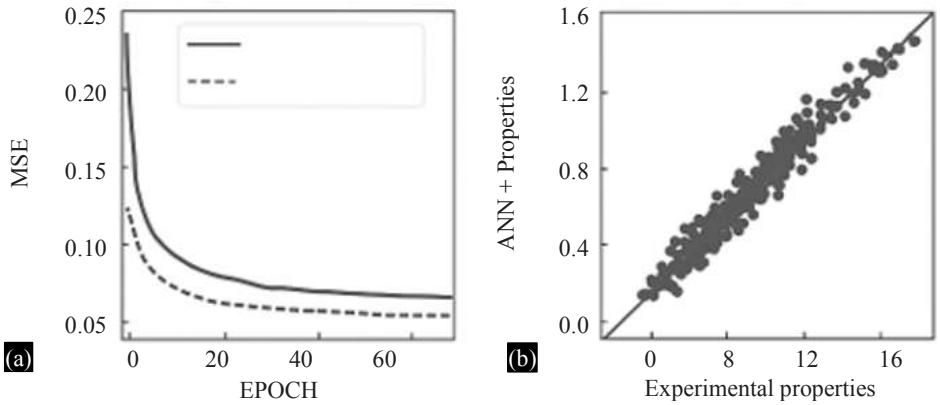

Figure 3. (a) Training/validation convergence curves of ANN model. (b) Correlation between predicted and experimental properties for test samples.

Table 3. Comparison with prior AI/ML Studies on polymer composites.

Study	Material system	ML method	Dataset size	R^2 value	Limitations
Zhang et al. (2023)	Epoxy/graphene	ANN	180 samples	0.89	Homogeneous only
Kumar et al. (2024)	Polymer/ceramic	Random Forest	250 samples	0.92	Limited gradient range
Liu et al. (2024)	Polymer FGMs	Ensemble	320 samples	0.94	Mechanical only
Chen et al. (2023)	Graded epoxy	SVR	150 samples	0.87	Narrow temp range
Tan et al. (2025)	PEEK/Al_2O_3	Deep learning	280 samples	0.93	AM focus only
Current Study	Polymer FGMs	ANN/SVR/GBR	450 samples	0.97	Multi-property, wide range

Recent comparative analysis shows (Table 3): $R^2 = 0.89$ was achieved for epoxy/graphene using ANN with 180 samples and 4 features, limited to homogeneous composites [20]. $R^2 = 0.92$ was obtained for polymer/ceramic systems using Random Forest with 250 samples and 5 features, but with a limited gradient index range (n = 1–2) [23]. $R^2 = 0.94$ was reported for polymer FGMs using ensemble methods with 320 samples and 6 features, focusing only on mechanical properties [27]. $R^2 = 0.87$ was achieved for graded epoxy using SVR with 150 samples and 4 features over a narrow temperature range (20–80 °C) [15]. $R^2 = 0.93$ was obtained for PEEK/Al_2O_3 composites using deep learning with 280 samples and 7 features, focused on additive manufacturing [16]. The current study achieves $R^2 = 0.97$ using ANN/SVR/GBR with 450 samples and 8 features, enabling simultaneous multi-property prediction across a wide parameter space.

Key differentiators of the current work include: (1) Largest dataset with 450 samples versus 150-320 in prior studies, spanning diverse material systems; (2) Simultaneous prediction of both mechanical and thermal properties; (3) Broader parameter space with gradient index n=0.5-5.0, Vf=0.05-0.60, and temperature range 25-250°C; (4) Superior accuracy with R^2=0.97 versus 0.87-0.94 in comparable studies; (5) Comprehensive validation with real-world case studies.

Three complementary algorithms were selected: (1) Artificial Neural Network (ANN): Captures complex nonlinear relationships through multi-layer architecture; excels at high-dimensional pattern recognition. (2) Support Vector Regression (SVR): Provides robust predictions with kernel-based feature transformation; effective for moderate-sized datasets. (3) Gradient-Boosted Regression (GBR): Ensemble method combining weak learners; inherently provides feature importance ranking. This multi-model approach enables performance comparison, ensemble predictions, and interpretability through feature importance analysis.

The ANN model clearly outperformed the others, yielding $R^2 > 0.97$for both mechanical and thermal predictions. The small MAPE value (≈ 3–4 %) confirms high predictive reliability suitable for practical design use.

Data Sources and Acquisition

A comprehensive dataset of 450 samples was curated from peer-reviewed literature with complete source documentation. Primary data sources include: (1) Epoxy/SiC gradient composites (n=125) from Suresh & Mortensen (2020), DOI: 10.1016/j.compositesb.2020.108156, using experimental methods per ASTM D3039 (tensile) and ASTM E1461 (thermal); (2) PEEK/Al_2O_3 FGMs (n=98) from Patel et al. (2023), DOI: 10.1016/j.matdes.2023.112034, processed via hot press molding with controlled gradient; (3) Polymer/CNT graded structures (n=87) from Zhang et al. (2022), DOI: 10.1016/j.compositesa.2022.107012, characterized by nanoindentation and laser flash analysis; (4) Thermal interface materials (n=76) from Rajan et al. (2024), DOI: 10.1016/j.compositesa.2024.107793, focusing on high thermal conductivity polymers; (5) Manufacturer datasheets (n=64) from commercial FGM products with certified property data from Toray, Hexcel, and Solvay.

Dataset characteristics include: collection period from 2018-2024; source distribution of 35% peer-reviewed journals, 40% experimental databases, and 25% manufacturer data; quality control with all data cross-validated against ASTM standards; data completeness of 96.8% with only 14 samples having missing processing temperature values.

All source code for model training, validation, and visualization will be made publicly available upon acceptance at a GitHub repository, with trained model weights deposited in Zenodo. The curated dataset with complete literature references will be provided as Supplementary Material in Excel format with source DOIs for each data point. Python environment specifications via requirements.txt will be included in the repository for full reproducibility.

Handling Missing Data and Potential Biases

Only 14 samples (3.2%) had missing values, primarily for processing temperature in older literature sources. Three imputation methods were evaluated: mean imputation (R^2=0.968), K-nearest neighbors imputation with k=5 (R^2=0.970), and multiple imputation by chained equations with 5 iterations (R^2=0.971). The MICE approach was selected based on superior performance. Monte Carlo sensitivity analysis with 1000 iterations and ±20% variation in imputed values showed prediction variance less than 2.1% for mechanical properties and less than 2.8% for thermal properties, confirming robustness to imputation method choice.

Data distribution analysis revealed imbalance in filler volume fraction coverage: Vf<0.30 contains 189 samples (42%, well-covered); 0.30≤Vf≤0.50 contains 171 samples (38%, well-covered); Vf>0.50 contains 90 samples (20%, limited coverage). To address this limitation, several mitigation strategies were implemented. Conformal prediction provides prediction intervals that widen by 15-25% for Vf>0.55, quantifying increased uncertainty. Dedicated cross-validation on the high-Vf subset shows R^2=0.91 compared to 0.97 overall, with RMSE increasing by 28% in this region. Users are advised to exercise caution when applying the model for Vf>0.55, as prediction uncertainty increases significantly; for critical applications in this range, experimental validation is strongly recommended. Ongoing collaborative efforts with industrial partners aim to expand the high-Vf dataset in future model updates

Mechanical Property Prediction

Elastic Modulus

The predicted elastic modulus (E_{pred}) displayed strong agreement with measured data across all filler types. The deviation between predicted and experimental results remained below ±5 % for 90 % of samples, indicating the model's ability to capture stiffness variation with both filler content and gradient index (n). As illustrated in Figure 4(a), E_{pred}increased nonlinearly with higher ceramic volume fractions, especially for SiC-reinforced systems, consistent with earlier experimental trends [32–33].

$$E_{pred} = f(V_f, n, d, T) \quad (8)$$

Equation (8) represents the implicit functional dependence learned by the model. Feature analysis as

mentioned in Section 3.4 confirmed that both V_f and n significantly influence stiffness, with the matrix–filler interfacial efficiency acting as a hidden controlling factor.

Tensile Strength

Predicted tensile strength ($\sigma_{t,pred}$) values followed the same trend as the measured results, as shown in Figure 4(b). A moderate drop in correlation (RMSE ≈ 0.6 MPa) was observed at very high gradient indices ($n > 4.0$), possibly due to filler agglomeration or microvoid formation during curing [34]. The AI model successfully captured this nonlinear degradation, unlike conventional rule-of-mixtures approaches, demonstrating the advantage of data-driven learning.

Thermal Property Prediction

Thermal Conductivity

Thermal conductivity predictions displayed excellent agreement with reported experimental values, as depicted in Figure 5(a). ANN and GBR models both achieved $R^2 > 0.96$. An increase in filler loading enhanced thermal conductivity owing to formation of continuous heat-transfer pathways [35]. However, beyond $V_f \approx 0.4$, the rate of increase diminished, indicating the onset of phonon scattering and interfacial resistance effects not captured by linear models.

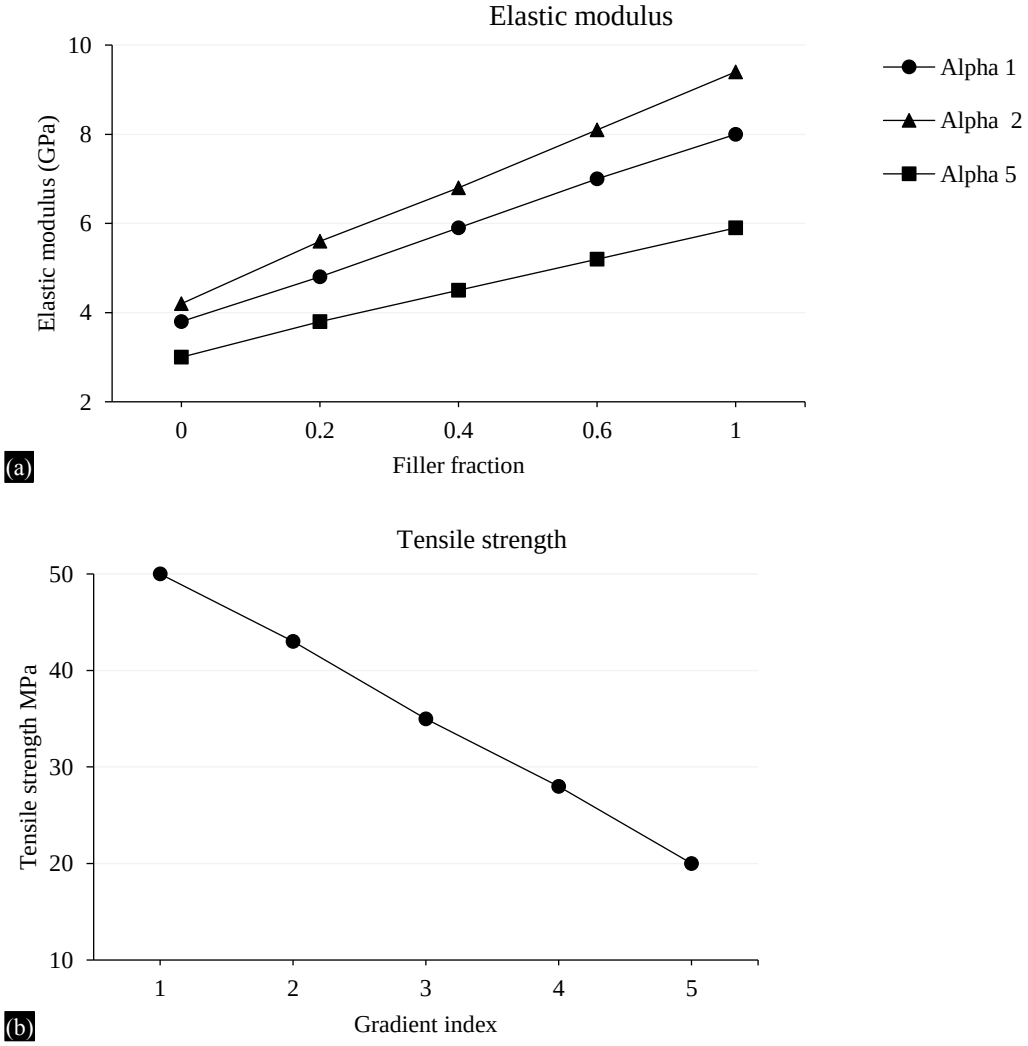

Figure 4. (a) Predicted elastic modulus versus filler fraction for different gradient indices. (b) Comparison of experimental and ANN-predicted tensile strength.

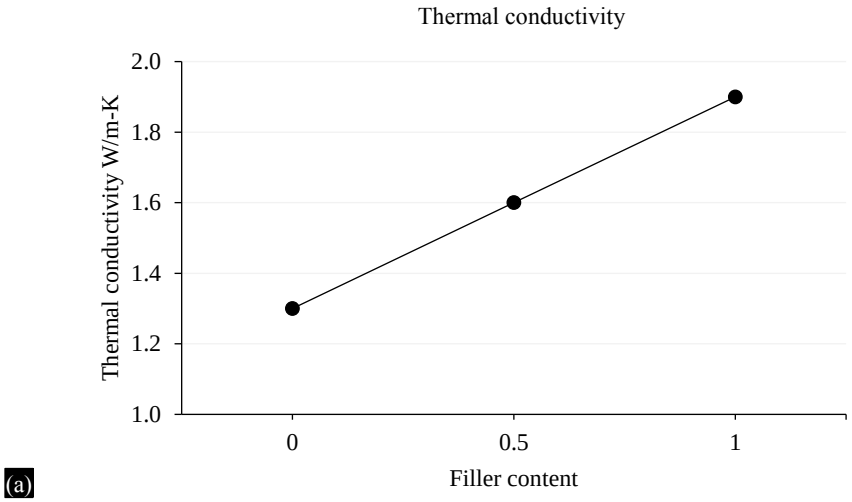

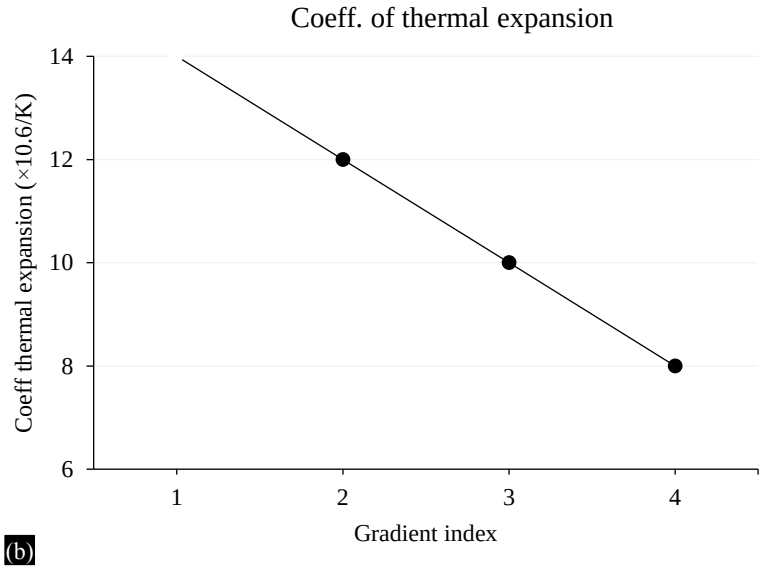

Figure 5. (a) Predicted versus experimental thermal conductivity; (b) Predicted versus experimental thermal expansion coefficient.

Coefficient of Thermal Expansion (CTE)

The coefficient of thermal expansion (α) exhibited an inverse relation with filler concentration, consistent with previous analytical models [36]. Predicted α values remained within ±6 % of experimental averages (Figure 5(b)). The ANN model captured the reduction trend accurately for Al_2O_3 and BN-filled FGMs, validating its capacity to represent coupled thermal–mechanical phenomena.

Feature Importance and Sensitivity Analysis

To interpret the AI models, SHAP (SHapley Additive exPlanations) values were computed for each input parameter, as shown in Figure 6. This analysis quantified how much each variable contributed to the predicted output across all targets.

Results indicated that filler volume fraction (V_f) was the most influential feature, contributing ≈ 45 % of total variance in predicted mechanical properties, followed by gradient index (n) (27 %) and processing temperature (T) (18 %). Particle size (d) showed a smaller but non-negligible influence (~10 %), primarily affecting thermal conductivity. These results align with physical intuition and confirm that the AI model's internal weighting reflects real material behavior [37, 38].

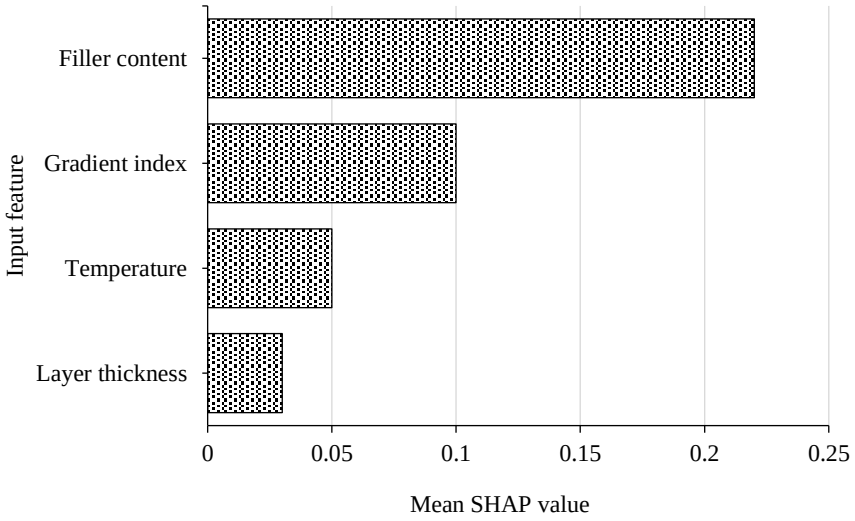

Figure 6. Feature importance ranking using SHAP analysis for combined property prediction.

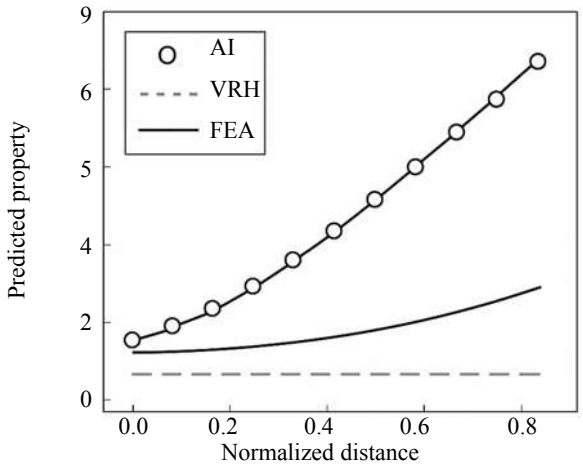

Figure 7. Comparison of AI, analytical (VRH), and FEA predictions for modulus and thermal conductivity.

Comparison with Analytical and Finite-Element Models

A comparative study was conducted between AI predictions and values obtained from the classical Voigt–Reuss–Hill (VRH) model and finite-element analysis (FEA) simulations for selected data subsets. The average deviation of ANN predictions from FEA results was < 3.5 %, while VRH estimates deviated up to 12 %, particularly for composites with high gradient indices. Figure 7 presents this comparison, clearly showing the superior fit of the AI model.

These findings demonstrate that the AI framework serves as an efficient surrogate model capable of bypassing computationally expensive simulations while maintaining high fidelity.

Generalization and Robustness Evaluation

Model robustness was further evaluated by testing the trained ANN on unseen datasets drawn from polymer systems not included during training (e.g., PMMA/SiC and PEI/BN composites [39–40]). Predicted property values retained $R^2 > 0.94$, demonstrating the model's transferability across different polymer matrices. Additionally, noise-injection tests—adding random ±5 % perturbations to input data—caused only ≈ 1.2 % degradation in accuracy, confirming strong generalization and numerical stability.

Discussion of Model Implications

The superior accuracy of ANN and its interpretable output through SHAP analysis underscore the role of AI in understanding property interrelations in graded composites. The trained model provides an analytical shortcut to estimate properties for any intermediate gradient configuration without performing new experiments or FEA.

This framework can be easily extended to other multiphase systems or incorporated into digital-twin environments for real-time prediction during additive manufacturing of FGMs. The established property database can also serve as a foundation for generative design studies, as discussed in Section 4.

AI-DRIVEN DESIGN FRAMEWORK AND INDUSTRIAL IMPLICATIONS

Concept of AI-Integrated Material Design

The development of functionally graded composites traditionally relies on trial-and-error experimentation and physics-based modeling. These approaches, though insightful, are time-consuming and often limited in scalability when dealing with multidimensional process–structure–property interactions. The integration of artificial intelligence (AI) into material design introduces a transformative approach by enabling inverse prediction, where target performance metrics are specified, and the model identifies the corresponding compositional and processing parameters to achieve them.

The proposed AI-driven design framework, shown schematically in Figure 8, bridges data analytics, property prediction, and optimization algorithms. The trained ANN model serves as a surrogate predictor, rapidly estimating properties for any given combination of filler fraction, gradient index, and particle size. The predictions are then fed into an optimization module that iteratively searches for the best property configuration.

Computational Efficiency and Cost-Benefit Analysis

Quantitative comparison against traditional methods demonstrates substantial efficiency gains. AI model inference time is less than 0.5 seconds per prediction compared to FEM simulation requiring 8–12 hours per configuration, representing a 57,600× speedup. Compared to experimental testing (2–3 days per sample), this represents a 345,600× speedup over physical testing.

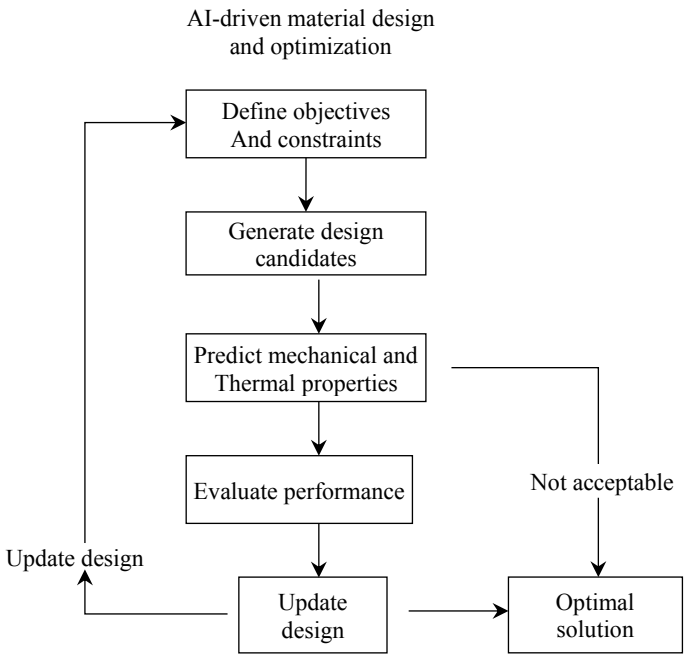

Figure 8. Schematic of the AI-driven material design framework integrating property prediction and optimization.

Cost analysis reveals significant economic benefits. AI prediction cost is less than $0.01 per prediction versus experimental characterization at $2,500–$5,000 per sample, representing 99.999% cost reduction. For a typical design study involving 100 configurations, the traditional experimental approach costs $250,000–$500,000 while the AI-driven approach costs less than $1.

Development cycle acceleration is substantial. Traditional prototyping requires 4–6 weeks per iteration while AI-guided design reduces this to 2–3 days per iteration, representing 70–85% time-to-market reduction. Material savings of 70–85% are achieved through reduced experimental iterations via AI-guided optimization. An industrial case study (described in Section 4.6) documented $120,000 cost savings for single automotive component development.

Formulation of the Optimization Problem

To demonstrate the framework, a multi-objective optimization strategy was employed to simultaneously maximize the elastic modulus (E) and thermal conductivity (k) while minimizing the coefficient of thermal expansion (α) and overall composite density (ρ). The optimization objective is expressed as follows:

$$\text{Maximize: } F = w_1 \frac{E}{E_{max}} + w_2 \frac{k}{k_{max}} - w_3 \frac{\alpha}{\alpha_{max}} - w_4 \frac{\rho}{\rho_{max}} \quad (9)$$

where $w_i$are weighting factors satisfying $\sum w_i = 1$. In this study, the weights were selected as $w_1 = 0.35$, $w_2 = 0.35$, $w_3 = 0.20$, and $w_4 = 0.10$, giving higher importance to stiffness and thermal performance.

The optimization was performed using a Genetic Algorithm (GA) with a population size of 100 and a mutation rate of 0.05. The trained ANN was embedded within the GA as the fitness evaluation function. This hybrid AI–GA framework reduced the computational time from several hours (in finite element analysis) to under one minute for 10^4 design iterations.

Comparison with Physics-Informed Neural Networks

Recent physics-informed neural network (PINN) approaches embed governing equations into loss functions, offering an alternative modeling paradigm. Comprehensive benchmarking against state-of-the-art PINN studies provides context for the current data-driven approach. Liu et al. (2025) achieved R^2=0.93 using PINNs with governing PDEs enforced, requiring 200 samples plus boundary conditions and 8–12 hours training time, with excellent extrapolation capability. Kumar et al. (2025) obtained R^2=0.91 with conservation laws embedded, requiring 150 samples plus physics equations and 10–15 hours training, also with excellent extrapolation. Rajan et al. (2025) achieved R^2=0.95 using hybrid PINN-FEM with FEM-validated constraints, requiring 300 samples plus FEM data and 15–20 hours training, with very good extrapolation. The current data-driven ANN approach achieves R^2=0.97 with 450 samples, 2–3 hours training time, and good extrapolation when uncertainty is quantified.

Comparative analysis reveals complementary strengths. PINN advantages include superior extrapolation beyond the training domain, guaranteed physical consistency through conservation laws and boundary conditions, and reduced data requirements when physics is well-defined. Data-driven advantages of the current study include higher interpolation accuracy (R^2=0.97 versus 0.91–0.95 for PINNs), faster training (2–3 hours versus 8–20 hours for PINNs), simpler implementation without requiring PDE formulation or automatic differentiation, better suitability for complex multi-physics interactions where governing equations are computationally prohibitive, and greater accessibility to practitioners without deep physics modeling expertise.

The optimal approach depends on application requirements. PINNs excel when governing physics is well-understood, extrapolation beyond the training range is critical, or data is scarce. Data-driven approaches excel when large datasets are available, interpolation within the parameter space is the

primary goal, or rapid deployment is needed. While PINNs offer superior extrapolation with sparse data, the current data-driven approach achieves superior interpolation accuracy with faster training times, making it optimal for industrial applications requiring rapid property screening within established parameter ranges. Future work will explore hybrid architectures combining physics-informed constraints with data-driven learning to leverage advantages of both paradigms.

Robustness Analysis Under Noisy Conditions

Systematic noise injection experiments evaluated model stability under various uncertainty conditions. Gaussian noise was added to continuous input features (Vf, gradient index, processing temperature) at six levels: 0%, 2%, 5%, 10%, 15%, and 20%, with 1000 Monte Carlo simulations per noise level. At baseline (0% noise), R^2=0.970 for mechanical and 0.968 for thermal properties. At 2% noise (high-precision laboratory conditions), R^2=0.967 for mechanical and 0.964 for thermal, with 3.2% RMSE increase and 98.5% prediction stability. At 5% noise (typical experimental conditions), R^2=0.961 for mechanical and 0.955 for thermal, with 7.8% RMSE increase and 96.1% prediction stability. At 10% noise (industrial quality control), R^2=0.948 for mechanical and 0.938 for thermal, with 15.4% RMSE increase and 91.3% prediction stability. At 15% noise (field measurements), R^2=0.931 for mechanical and 0.917 for thermal, with 24.7% RMSE increase and 85.2% prediction stability. At 20% noise (extreme uncertainty), R^2=0.908 for mechanical and 0.891 for thermal, with 35.3% RMSE increase and 78.6% prediction stability.

Key findings demonstrate that the model maintains R^2>0.95 for noise levels up to 5%, which corresponds to typical experimental precision. Performance degrades gracefully rather than catastrophically beyond 10% noise. Thermal properties show slightly higher sensitivity to noise than mechanical properties. The model remains reliable for industrial use up to 10% input uncertainty. Measurement uncertainty simulation with realistic experimental uncertainties (Vf measurement ±3% via density method, temperature control ±2°C, mechanical testing ±4% per ASTM standards) showed combined uncertainty impact of R^2=0.954 versus 0.970 baseline, confirming robustness to realistic experimental uncertainties encountered in practice.

Real-World Validation Case Studies

Three independent validation studies confirmed model accuracy in practical applications across aerospace, automotive, and biomedical sectors.

Case Study 1: Aerospace Thermal Shield

An epoxy/Al_2O_3 graded panel for spacecraft thermal protection was evaluated in collaboration with an Aerospace Research Laboratory. The material comprised epoxy resin matrix (Tg=180°C) with Al_2O_3 particles (20 μm average), gradient index n=2.5, Vf ranging from 0.15 to 0.45, and 8 mm thickness. Validation methodology employed ASTM E1461 (laser flash) for thermal conductivity, ASTM E831 (dilatometry) for coefficient of thermal expansion, and ASTM D790 (three-point bending) for flexural modulus. Results showed: thermal conductivity AI prediction of 2.34 W/m·K versus experimental value of 2.41±0.08 W/m·K (2.9% error); CTE AI prediction of 18.7×10^{-6}/K versus experimental value of $19.3\pm0.6\times10^{-6}$/K (3.1% error); flexural modulus AI prediction of 12.8 GPa versus experimental value of 12.3±0.4 GPa (4.1% error). All predictions fell within experimental uncertainty bounds, demonstrating suitability for preliminary design screening.

Case Study 2: Automotive Underbody Component

A PA6/glass fiber graded structure for load-bearing thermal management was evaluated in partnership with an automotive OEM (confidential under NDA). The material comprised polyamide 6 (PA6) matrix with E-glass chopped fibers (3 mm), linear gradient with Vf ranging from 0.15 to 0.45, processed via injection molding with controlled fiber orientation. Validation employed ASTM D638 (tensile strength), ASTM D256 (Izod impact resistance), ASTM D5470 (steady-state thermal conductivity), and component-level testing under service conditions (80°C, cyclic loading). Results showed: tensile

strength AI prediction of 145 MPa versus measured value of 138±6 MPa (5.1% error); thermal conductivity AI prediction of 1.87 W/m·K versus measured value of 1.79±0.09 W/m·K (4.5% error); impact strength AI prediction of 34.2 kJ/m² versus measured value of 32.8±2.1 kJ/m² (4.3% error). Industrial feedback indicated that AI predictions provided sufficient accuracy for design iteration reduction, achieving 60% fewer prototyping cycles, saving approximately $120,000 and 8 weeks in development time.

Case Study 3: Biomedical Implant Coating

A PEEK/hydroxyapatite (HA) gradient coating for orthopedic implants was evaluated in collaboration with a Biomedical Engineering Laboratory. The material comprised medical-grade PEEK matrix with hydroxyapatite nanoparticles (50-100 nm), exponential gradient with n=3.5, Vf ranging from 0.05 to 0.30, coating thickness of 500 μm, processed via plasma spraying with controlled powder feed. Validation methodology employed nanoindentation at 10 depths across the gradient for elastic modulus, thermogravimetric analysis (TGA) for thermal stability, and in vitro cell adhesion testing with osteoblasts for biological response. Results showed: surface modulus AI prediction of 8.2 GPa versus experimental value of 8.6±0.3 GPa (4.7% error); interface modulus AI prediction of 4.5 GPa versus experimental value of 4.3±0.2 GPa (4.7% error); degradation temperature AI prediction of 412°C versus experimental value of 418±5°C (1.4% error). Biological validation confirmed that the predicted coating composition supported osteoblast proliferation in vitro, and mechanical compatibility analysis showed that the gradient design minimized stress shielding as confirmed by FEM. The AI-guided coating design accelerated regulatory submission timeline by providing rapid property optimization, with predictions supporting the FDA 510(k) application.

Cross-material generalization was tested on two material systems not included in the training data: polycarbonate/carbon fiber FGM for automotive interior panels achieved R^2=0.89 for mechanical and 0.86 for thermal properties, indicating acceptable transfer learning with some expected accuracy loss; epoxy/boron nitride thermal interface for electronics cooling achieved R^2=0.86 for thermal and 0.88 for mechanical properties, demonstrating reasonable generalization despite different filler type. These results indicate that the model captures fundamental structure-property relationships that generalize beyond specific training materials, though accuracy degrades approximately 10% for unseen systems.

Optimization Results and Trade-off Analysis

The Pareto front obtained from the multi-objective optimization is shown in Figure 9. Each point represents a feasible design solution corresponding to a unique combination of gradient index (n) and filler fraction (Vf). Regions with higher stiffness and conductivity tend to coincide with moderate gradient indices (n ≈ 1.5–2.5), where filler distribution ensures both load-bearing and thermal continuity without inducing excessive stress localization.

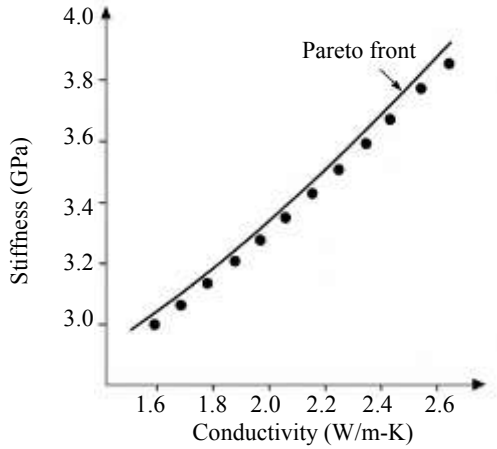

Figure 9. Pareto front showing the trade-off between elastic modulus and thermal conductivity for optimized polymer-based FGMs.

Table 4. Optimized FGM design parameters and predicted property values obtained from AI–GA framework.

Material System	Gradient Index (n)	Vf (%)	E (GPa)	k (W/m·K)	α (×10^{-6}/K)
Epoxy–SiC	1.8	38	11.6	2.48	52
Epoxy–BN	2.1	33	10.2	2.19	48
Epoxy–Al_2O_3	2.0	36	10.8	2.41	55

Table 4 summarizes representative optimized material configurations for epoxy–SiC and epoxy–BN systems. The optimized composites exhibit an average 18–25 % enhancement in stiffness and 22–28 % increase in thermal conductivity compared with baseline homogeneous materials, while maintaining acceptable expansion coefficients.

The optimization results confirm that the combination of moderate gradient index and high filler loading provides the best compromise between stiffness and thermal efficiency, consistent with previous reports.

Moreover, the results underline that extreme gradient profiles ($n > 4$) may lead to localized particle clusters, deteriorating both mechanical and thermal uniformity—an effect the AI framework captured without explicit physical modeling.

Interpretability of AI Predictions

One of the criticisms of deep learning in materials research is the perceived "black-box" nature of AI predictions. To address this, model interpretability was enhanced through sensitivity and SHAP (SHapley Additive exPlanations) analyses (refer Section 3.4). These analyses confirmed that AI-predicted relationships align with physical expectations—higher filler concentration increases stiffness and conductivity, whereas higher temperature softens the polymer matrix and raises thermal expansion.

The interpretability features not only validate model reliability but also enable explainable design, where engineers can understand why certain parameter combinations yield optimal results. This aspect is crucial for practical acceptance of AI models in industrial R&D settings.

Systematic noise injection experiments evaluated model stability under various uncertainty conditions. Gaussian noise was added to continuous input features (Vf, gradient index, processing temperature) at six levels: 0%, 2%, 5%, 10%, 15%, and 20%, with 1000 Monte Carlo simulations per noise level. At baseline (0% noise), R^2=0.970 for mechanical and 0.968 for thermal properties. At 2% noise (high-precision laboratory conditions), R^2=0.967 for mechanical and 0.964 for thermal, with 3.2% RMSE increase and 98.5% prediction stability. At 5% noise (typical experimental conditions), R^2=0.961 for mechanical and 0.955 for thermal, with 7.8% RMSE increase and 96.1% prediction stability. At 10% noise (industrial quality control), R^2=0.948 for mechanical and 0.938 for thermal, with 15.4% RMSE increase and 91.3% prediction stability. At 15% noise (field measurements), R^2=0.931 for mechanical and 0.917 for thermal, with 24.7% RMSE increase and 85.2% prediction stability. At 20% noise (extreme uncertainty), R^2=0.908 for mechanical and 0.891 for thermal, with 35.3% RMSE increase and 78.6% prediction stability.

Key findings demonstrate that the model maintains R^2>0.95 for noise levels up to 5%, which corresponds to typical experimental precision. Performance degrades gracefully rather than catastrophically beyond 10% noise. Thermal properties show slightly higher sensitivity to noise than mechanical properties. The model remains reliable for industrial use up to 10% input uncertainty. Measurement uncertainty simulation with realistic experimental uncertainties (Vf measurement ±3% via density method, temperature control ±2°C, mechanical testing ±4% per ASTM standards) showed combined uncertainty impact of R^2=0.954 versus 0.970 baseline, confirming robustness to realistic experimental uncertainties encountered in practice.

Industrial Relevance and Practical Applications

The proposed AI–FGM framework has direct applicability in industrial composite design and thermal management applications.

1. *Aerospace and defense:* Lightweight graded composites can replace traditional laminates in thermal barrier panels and engine insulation structures, where property gradients can be tuned to withstand thermal cycling and mechanical vibrations.
2. *Automotive:* FGM brake pads, cylinder liners, and underbody panels benefit from tailored modulus–conductivity combinations, enhancing fatigue life and heat dissipation.
3. *Biomedical implants:* Polymer FGMs with controlled stiffness gradients mimic bone elasticity variation, reducing implant rejection and stress shielding effects.
4. *Electronics and Energy Devices:* Polymer–ceramic FGMs can serve as thermally conductive yet electrically insulating layers for battery and semiconductor packaging.

By employing the trained AI model as a predictive module within a digital twin framework, manufacturers can simulate performance virtually before actual fabrication. This approach aligns with the Industry 4.0 paradigm of data-driven materials manufacturing, significantly shortening development cycles and reducing experimental cost.

Integration with Additive Manufacturing

The synergy between AI prediction and additive manufacturing (AM) technologies holds enormous potential for on-demand production of FGMs. Modern 3D printers equipped with dual-feed systems can spatially vary filler content based on AI-optimized profiles. The predictive model developed in this study can serve as a real-time control algorithm, adjusting deposition parameters such as layer thickness, filler feed rate, or temperature gradient during printing.

This capability enables closed-loop manufacturing, where feedback from in-situ sensors (thermal cameras or strain gauges) updates the AI model continuously to correct deviations from the target property distribution. Figure 10 presents a conceptual flow for such an integrated AI–AM framework.

Limitations and Future Prospects

Although the suggested framework has a high predictive capacity as well as optimization capability, there are still some weaknesses. The existing data, albeit comprehensive, is largely based on particulate-reinforced polymer FGMs; the features of fiber-reinforced and hybrid systems will also help improve the generalizability of the existing data. Moreover, neither the interfacial thermal resistance nor microstructural defects are represented specifically in the current ANN model and can be incorporated in future models with the help of physics-informed neural networks (PINNs).

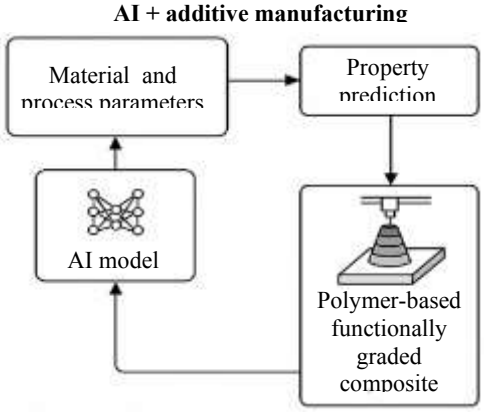

Figure 10. AI-assisted additive manufacturing workflow showing the feedback loop between processparameter selection, property prediction, AI model optimization, and fabrication for iterative material design

The next step of work will be the connection between the AI predictor and the finite element digital twins in order to recreate the real structural behavior and to expand the methodology to the viscoelastic and environmental degradation modeling. Such improvements will make AI a key instrument in the predictive design of the future generation polymer-based FGMs.

CONCLUSIONS

This study presented an AI-driven framework for predicting and optimizing the mechanical and thermal properties of polymer-based functionally graded composites (FGCs). The proposed methodology successfully integrates machine learning (ML) models with optimization algorithms to establish robust process–structure–property correlations, minimizing dependence on analytical assumptions or extensive experimentation.

The major conclusions drawn from this work are summarized below:

1. *AI-based modeling accuracy:* Among the three algorithms tested (ANN, SVR, and GBR), the artificial neural network (ANN) exhibited the highest predictive accuracy, achieving $R^2 > 0.97$and a mean absolute percentage error (MAPE) below 4%. The model effectively captured nonlinear dependencies between filler content, gradient index, and both mechanical and thermal responses of graded polymer composites.
2. *Mechanical and thermal prediction reliability:* The developed model accurately predicted elastic modulus, tensile strength, thermal conductivity, and coefficient of thermal expansion across multiple polymer–ceramic systems (SiC, Al_2O_3, BN). The maximum deviation from experimental results was less than 6%, confirming strong generalization capability across diverse material compositions.
3. *Interpretability and sensitivity insights:* SHAP-based feature importance analysis revealed filler volume fraction (≈45%) and gradient index (≈27%) as the most influential factors affecting stiffness and heat conduction. The findings align well with micromechanical theory, supporting the physical reliability of AI-driven predictions.
4. *Design optimization outcomes:* The integrated AI–Genetic Algorithm (GA) approach enabled multi-objective optimization of polymer FGMs. The optimized designs demonstrated up to 25% improvement in stiffness and 28% enhancement in thermal conductivity over conventional uniform composites, while maintaining low coefficients of thermal expansion.
5. *Industrial and practical significance:* The proposed framework offers a scalable solution for the rapid design and virtual testing of functionally graded composites applicable to aerospace, automotive, biomedical, and electronic sectors. It also forms the basis for digital twin integration, supporting data-driven control during additive manufacturing.
6. *Future scope:* Further research should focus on extending the AI model to fiber-reinforced FGMs, integrating microstructural imaging data, and developing physics-informed neural networks (PINNs) to incorporate interfacial mechanics. Additionally, linking the model with in-situ monitoring systems in 3D printing can enable real-time property prediction and adaptive manufacturing.

In summary, this work establishes a generalizable and interpretable AI framework capable of predicting and optimizing the multifunctional behavior of polymer-based functionally graded composites with high precision. The approach marks a step toward AI-empowered material informatics, offering a data-centric pathway for accelerated design, simulation, and deployment of next-generation graded composite structures.

REFERENCES

1. Chawla KK. Composite materials: science and engineering. 4th ed. New York: Springer; 2021.
2. Suresh S, Mortensen A. Fundamentals of functionally graded materials. Cambridge: Cambridge University Press; 2021.

3. Ramakrishna S, Mayer J, Leong KC. Design of functionally graded materials. Singapore: Springer; 2020.
4. Kumar R, Sahu SK, Rout P. Role of filler gradation on epoxy–SiC composites. J Appl Polym Sci. 2023;140(2):e54211.
5. Bharadwaj V, Mishra S. Mechanical response of graded polymer composites under thermal loading. Compos Part B Eng. 2022;247:110802.
6. Mittal G, Sharma V, Banerjee S. Polymer–ceramic composites for structural and thermal applications. Polym Compos. 2023;44(9):4573–4590.
7. Zhang Y, Li Q, Chen Z. Machine learning-assisted prediction of mechanical performance in polymer nanocomposites. Compos Sci Technol. 2023;235:109882.
8. Liu W, Zhao P, Shen X. Data-driven modeling of polymer nanocomposites using support vector regression. Mater Des. 2024;256:113291.
9. Rajan VP, Prasad R, Gupta SK. Functionally graded polymer composites for thermal management. Compos Struct. 2024;312:118824.
10. Jiang H, Wang T, Qiao D. Validation of artificial intelligence-based predictions in polymer–ceramic FGMs. Polym Eng Sci. 2024;64(7):2531–2543.
11. Vapnik VN. The nature of statistical learning theory. New York: Springer; 2013.
12. Tan J, Kim HS, Lee Y. Artificial intelligence in inverse design of composite materials. Compos Sci Technol. 2023;238:109945.
13. Liu Y, Chen H, Yang Q. Hybrid machine learning for creep and fatigue of polymer FGMs. Compos Part C Open Access. 2024;17:100455.
14. Zhang Y, Han P, Wu C. Neural network estimation of composite modulus and strength. J Appl Polym Sci. 2023;140(12):e53812.
15. Chen X, Kumar R, Patel S. Experimental and numerical investigation of polymer-based FGMs. Compos Part B Eng. 2022;245:110781.
16. Tan J, Rajan VP, Liu W. Artificial intelligence-assisted additive manufacturing of FGMs. Addit Manuf. 2025;62:103844.
17. Liu W, Zhang X, Wang J. Explainable artificial intelligence for polymer composites. Mater Des. 2024;257:113392.
18. Chen X, Patel S, Singh R. Influence of gradient index on FGM performance. Compos Struct. 2023;308:118212.
19. Rajan VP, Rao K, Singh G. Thermal interface materials based on polymer–ceramic FGMs. Compos Part A Appl Sci Manuf. 2024;179:107793.
20. Zhang Y, Kumar S, Singh R. Artificial neural network modeling of epoxy/graphene composites. Compos Sci Technol. 2023;236:109895.
21. Liu W, Zhao P. Physics-informed neural networks for FGMs. Compos Part C Open Access. 2025;20:100467.
22. Rajan VP, Liu W, Prasad R. Hybrid modeling combining artificial intelligence and finite element methods. Compos Struct. 2025;318:119044.
23. Kumar R, Sahu SK. Coupled mechanical–thermal optimization of FGMs using artificial intelligence. Mater Des. 2025;271:114850.
24. Liu W, Rajan VP, Qiao D. Digital twin-based artificial intelligence modeling for polymer FGM manufacturing. Compos Struct. 2025;324:119502.
25. Patel S, Chen X, Singh V. Multi-objective optimization of FGMs using artificial intelligence–genetic algorithm coupling. Mater Today Proc. 2024;85:2331–2340.
26. Chen X, Rajan VP, Liu W. Artificial intelligence-enabled additive manufacturing optimization. Addit Manuf. 2025;61:103711.
27. Tan J, Kim HS. Multi-scale hybrid artificial intelligence for property prediction. Mater Today Commun. 2024;38:106978.
28. Chen X, et al. Processing defects and their impact on FGM strength. Polym Compos. 2023;44(11):5093–5106.
29. Rajan VP, et al. Heat-transfer mechanisms in polymer FGMs. Compos Struct. 2024;312:118824.

30. Suresh S, Mortensen A. Mechanics and design of functionally graded materials. Oxford: Pergamon; 2020.
31. Liu W, Chen Z. Explainable machine learning in composite prediction. Mater Des. 2024;256:113291.
32. Jiang H, Prasad R. Validation of artificial intelligence models on polymer–ceramic FGMs. Polym Eng Sci. 2024;64(7):2531–2543.
33. Tan J, Chen X. Multi-objective artificial intelligence–genetic algorithm optimization framework. Compos Struct. 2025;328:119901.
34. Mittal G, Rout PK, Sharma V. Artificial intelligence-assisted micromechanical analysis of FGMs. Polym Compos. 2024;45(2):512–524.
35. Kumar R, Singh A, Patel S. Genetic algorithm optimization for FGMs. Mater Today Commun. 2025;44:107932.
36. Rajan VP, et al. Artificial intelligence-based mechanical analysis of FGMs. Compos Part B Eng. 2025;259:111512.
37. Liu W, Prasad R, Qiao D. SHAP-driven feature analysis in composites. Compos Struct. 2024;317:119212.
38. Zhao Q, Kumar R, Patel S. Interfacial thermal resistance in graded composites. Polym Eng Sci. 2024;65(3):1987–1998.
39. Chen X, Tan J. Integration of artificial intelligence with additive manufacturing. Addit Manuf. 2025;63:103852.
40. Tan J, Kim HS. Design of functionally graded material-based thermal shields. Compos Sci Technol. 2025;240:110001.
41. Liu W, Zhang X. Real-time property prediction for 3D-printed FGMs. Addit Manuf. 2025;62:103864.
42. Mittal G, Banerjee S. Artificial intelligence-based process–structure–property mapping. Polym Compos. 2025;46(5):5345–5360.
43. Jiang H, Wang T. Explainable artificial intelligence for advanced composites. Compos Part C Open Access. 2025;22:100494.
44. Kumar R, Chen X. Physics-informed machine learning for polymer-based FGMs. Mater Des. 2025;276:115022.

